J|A|C|S ARTICLES

Published on Web 08/27/2010

Nanomechanics of Lipid Bilayers: Heads or Tails?

Sergi Garcia-Manyes,*[,†,‡] Lorena Redondo-Morata,[‡,§,#] Gerard Oncins,[⊥] and Fausto Sanz*[,‡,§,#]

Department of Biological Sciences, Columbia University, New York, 10027, New York, Departament de Química Física, Universitat de Barcelona, 08028, Spain, Institut de Bioenginyeria de Catalunya, Barcelona, 08028, Spain, Serveis Cientificotècnics, Universitat de Barcelona, 08028, Spain, and CIBER-BBN, Zaragoza 50018, Spain

Received January 19, 2010; E-mail: sergi@biology.columbia.edu; fsanz@ub.edu

Abstract: Understanding the effect of mechanical stress on membranes is of primary importance in biophysics. Here we use force spectroscopy AFM to quantitatively characterize the nanomechanical stability of supported lipid bilayers as a function of their chemical composition. The onset of plastic deformation reveals itself as a repetitive jump in the approaching force curve, which represents a molecular fingerprint for the bilayer mechanical stability. By systematically probing a set of chemically distinct supported lipid bilayers (SLBs), we first show that both the headgroup and tail have a decisive effect on their mechanical properties. While the mechanical stability of the probed SLBs linearly increases by 3.3 nN upon the introduction of each additional $-CH_2-$ in the chain, it exhibits a significant dependence on the phospholipid headgroup, ranging from 3 nN for DPPA to 66 nN for DPPG. Furthermore, we also quantify the reduction of the membrane mechanical stability as a function of the number of unsaturations and molecular branching in the chemical structure of the apolar tails. Finally, we demonstrate that, upon introduction of cholesterol and ergosterol, contrary to previous belief the mechanical stability of membranes not only increases linearly in the liquid phase (DLPC) but also for phospholipids present in the gel phase (DPPC). Our results are discussed in the framework of the continuum nucleation model. This work highlights the compelling effect of subtle variations in the chemical structure of phospholipid molecules on the membrane response when exposed to mechanical forces, a mechanism of common occurrence in nature.

Introduction

The diversity in the chemical composition of the ample phospholipid repertoire is intricately related to biomembrane lateral organization[1,2] and function.[3,4] In particular, membrane mechanics, which plays a crucial role in endo- and exocytosis, and also in determining the cell shape,[5] strongly depends on the membrane chemical composition. Two main types of model systems, namely micrometer-sized free-standing membranes and supported planar lipid bilayers (SLBs), have been extensively used to mimic the biophysical properties of biological membranes.[6,7] In the latter case, the bilayers are generally adsorbed onto a planar hydrophilic substrate by Langmuir−Blodgett deposition or by fusion of small, unilamellar vesicles.[8,9] While the close presence to the solid substrate partially influences the properties of supported lipid bilayers by significantly inhibiting lipid mobility and limiting the insertion of transmembrane proteins,[10−13] they retain the basic thermodynamic and structural properties of free bilayers[14] with the advantage of being susceptible of investigation using highly sensitive and localized techniques.[7,15]

Several techniques have been employed to quantitatively investigate the mechanical properties of lipid bilayers. For example, photoelectron correlation spectroscopy, dynamic light scattering and cryoelectron microscopy have been used to study the behavior of vesicles under osmotic stress. The most

† Columbia University.
‡ Departament de Química Física, Universitat de Barcelona.
§ Institut de Bioenginyeria de Catalunya.
⊥ Serveis Cientificotècnics, Universitat de Barcelona.
CIBER-BBN.

(1) Miller, C. E.; Majewski, J.; Watkins, E. B.; Mulder, D. J.; Gog, T.; Kuhl, T. L. *Phys. Rev. Lett.* **2008**, *100*, 058103.
(2) Simons, K.; Vaz, W. L. *Annu. Rev. Biophys. Biomol. Struct.* **2004**, *33*, 269–295.
(3) Dowhan, W. *Annu. Rev. Biochem.* **1997**, *66*, 199–232.
(4) van Meer, G.; Voelker, D. R.; Feigenson, G. W. *Nat. Rev. Mol. Cell Biol.* **2008**, *9*, 112–124.
(5) Vogel, V.; Sheetz, M. *Nat. Rev. Mol. Cell Biol.* **2006**, *7*, 265–275.
(6) Watkins, E. B.; Miller, C. E.; Mulder, D. J.; Kuhl, T. L.; Majewski, J. *Phys. Rev. Lett.* **2009**, *102*, 238101.
(7) El Kirat, K.; Morandat, S.; Dufrene, Y. F. *Biochim. Biophys. Acta* **2010**, *1798*, 750–765.
(8) Brian, A. A.; McConnell, H. M. *Proc. Natl. Acad. Sci. U.S.A.* **1984**, *81*, 6159–6163.
(9) Watts, T. H.; Brian, A. A.; Kappler, J. W.; Marrack, P.; McConnell, H. M. *Proc. Natl. Acad. Sci. U.S.A.* **1984**, *81*, 7564–7568.
(10) Herold, C.; Schwille, P.; Petrov, E. P. *Phys. Rev. Lett.* **2010**, *104*, 148102.
(11) Scomparin, C.; Lecuyer, S.; Ferreira, M.; Charitat, T.; Tinland, B. *Eur. Phys. J., E* **2009**, *28*, 211–220.
(12) Goksu, E. I.; Nellis, B. A.; Lin, W. C.; Satcher, J. H., Jr.; Groves, J. T.; Risbud, S. H.; Longo, M. L. *Langmuir* **2009**, *25*, 3713–3717.
(13) Goksu, E. I.; Hoopes, M. I.; Nellis, B. A.; Xing, C.; Faller, R.; Frank, C. W.; Risbud, S. H.; Satcher, J. H., Jr.; Longo, M. L. *Biochim. Biophys. Acta* **2010**, *1798*, 719–729.
(14) Sackmann, E. *Science* **1996**, *271*, 43–48.
(15) Seantier, B.; Giocondi, M. C.; Le Grimellec, C.; Milhiet, P. E. *Curr. Opin. Colloid Interface Sci.* **2008**, *13*, 326–337.

 10.1021/ja1002185

outstanding approach, the micropipet aspiration technique,[16−18] has provided a wealth of information regarding quantitative values for membrane elastic moduli for area dilation, shear and bending.[19] While crucial, these experiments are mostly restricted to the use of giant vesicles, thus providing a 'mesoscopic' outlook on bilayer mechanical stability. Nonetheless, the broad chemical diversity of the cell membrane demands experimental techniques able to probe the local elastic properties of lipid bilayers with nanometer resolution.

At this length scale, the mechanical properties of individual lipid bilayers are best probed when they are supported onto solid substrates. Using this approach, the surface force apparatus (SFA) has provided valuable insight into the study of lipid bilayer adhesion, fusion and healing, allowing direct measurement of the interaction forces arising between symmetrical and asymmetrical supported lipid bilayers.[20−24] However, this technique is mostly limited to the study of the interaction between two facing bilayers, which are deposited onto two opposing mica surfaces. On the other hand, atomic force microscopy (AFM), which has emerged as an essential tool to investigate the topology of lipid bilayers,[15,25,26] has allowed the independent measurement of the local (nano)mechanical properties of individual supported lipid bilayers using the force spectroscopy mode operating under constant velocity.[27] Contrary to free-standing bilayers, where the intrinsic curvature determines the bending and stretching modes of elasticity,[13] the solid support constrains supported lipid bilayers to a planar o nearly planar geometry,[28] such that they can only be compressed in the vertical direction.[29] Such experimental approach provides the perfect platform to quantitatively study the in-plane chemical interactions that govern the nanomechanical stability of supported lipid bilayers. These force spectroscopy experiments have already offered a new perspective on membrane mechanics in a confined area within the nanometer realm, where most of the specific molecular interactions take place.[30−32] In particular, these experiments have demonstrated the effect of temperature[33,34] and ionic strength[35] on the nanomechanical properties of supported lipid bilayers (SLBs). More recently, they have allowed identification of phase separation on different mixtures of phospholipids.[36,37] Despite such impressive progress,[38] a systematic, comprehensive study relating phospholipid chemical composition and (nano)mechanical stability remains elusive.

Herein, we employ force spectroscopy on chemically distinct SLBs to quantitatively explore the molecular determinants that provide mechanical stability to the supported membrane. By systematically and independently changing the chemical composition of the hydrophilic head, the length of the hydrophobic tail, the number of chain unsaturations and the cholesterol concentration, we gain insights into the mechanical stability of each bilayer, which is a direct signature of membrane lateral organization. Our results demonstrate that the overall mechanical stability of the lipid bilayer results from a complex and fine mechanochemical balance, where the chemical composition of both the headgroup and tail has a crucial effect.

Materials and Methods

Sample Preparation. Phospholipid supported bilayers were prepared by small unilamellar bilayer deposition on freshly cleaved mica surface following the method described elsewhere[25,33,35] and further detailed in the Supporting Information section.

AFM Imaging. Phospholipid supported bilayers were imaged using a commercial 3D-MFP AFM (Asylum Research, Santa Barbara, CA) setup in tapping mode using V-shaped Si_3N_4 cantilevers (OMCL TR400PSA, Olympus) with a nominal spring constant of 80 pN/nm. The measurements were performed under constant temperature ranging from 19 and 21 °C.

Force Spectroscopy Measurements. Force spectroscopy measurements were conducted using 1D- and 3D-MFP AFM (Asylum Research, Santa Barbara, CA) set-ups. Prior to performing the force-curves, topographic images were acquired using the tapping mode. Images and force-plots were acquired using V-shaped Si_3N_4 cantilevers (OMCL TR400PSA, Olympus) with a nominal spring constant of 80 pN/nm. Individual spring constants were calibrated using the equipartition theorem. For SLBs exhibiting higher mechanical resistance, stiffer Veeco DNP cantilevers were employed (580 pN/nm). In all the experiments, the piezoelectric actuator was extended and retracted at the same constant velocity (1 μm s^{-1}). For each probed phospholipid SLB, at least three independent experiments with different cantilever/sample combination were conducted. The distribution of F_b values exhibits low scattering (<15%) when using different cantilever tips and samples within independent days of experiment. Further details are described in the Supporting Information section.

Results

Force Curves on SLBs Reveal a Breakthrough That Provides a True Molecular Fingerprint of the Membrane Mechanical Resistance. In our experiments, we deposit liposomes of small size onto a freshly cleaved mica substrate to form a continuous supported lipid bilayer (Figure 1). The formation of the bilayer is verified by imaging the surface in tapping mode. Such images reveal bilayers that typically extend more than 1 μm, exhibiting heights of ∼5 nm (Figure 1 B−C).

(16) Rawicz, W.; Olbrich, K. C.; McIntosh, T.; Needham, D.; Evans, E. *Biophys. J.* **2000**, *79*, 328–339.
(17) Evans, E.; Rawicz, W. *Phys. Rev. Lett.* **1990**, *64*, 2094–2097.
(18) Needham, D.; Zhelev, D. V. In *Vesicles*; Rosoff, M., Ed.; Marcel Dekker Inc.: New York, 1996; Vol. 62.
(19) Heinrich, V.; Rawicz, W. *Langmuir* **2005**, *21*, 1962–1971.
(20) Israelachvili, J. *Intermolecular and Surface Forces*; Academic Press: London, 1991.
(21) Marra, J.; Israelachvili, J. *Biochemistry* **1985**, *24*, 4608–4618.
(22) Marra, J. *Biophys. J.* **1986**, *50*, 815–825.
(23) Helm, C. A.; Israelachvili, J. N.; McGuiggan, P. M. *Science* **1989**, *246*, 919–922.
(24) Benz, M.; Gutsmann, T.; Chen, N.; Tadmor, R.; Israelachvili, J. *Biophys. J.* **2004**, *86*, 870–879.
(25) Mingeot-Leclercq, M. P.; Deleu, M.; Brasseur, R.; Dufrene, Y. F. *Nat. Protoc.* **2008**, *3*, 1654–1659.
(26) Goksu, E. I.; Vanegas, J. M.; Blanchette, C. D.; Lin, W. C.; Longo, M. L. *Biochim. Biophys. Acta* **2009**, *1788*, 254–266.
(27) Dufrene, Y. F.; Boland, T.; Schneider, J. W.; Barger, W. R.; Lee, G. U. *Faraday Discuss* **1998**, 79–94. Dufrene, Y. F.; Boland, T.; Schneider, J. W.; Barger, W. R.; Lee, G. U. *Faraday Discuss* **1998**, 137–157.
(28) Smith, H. L.; Jablin, M. S.; Vidyasagar, A.; Saiz, J.; Watkins, E.; Toomey, R.; Hurd, A. J.; Majewski, J. *Phys. Rev. Lett.* **2009**, *102*, 228102.
(29) Mey, I.; Stephan, M.; Schmitt, E. K.; Muller, M. M.; Ben Amar, M.; Steinem, C.; Janshoff, A. *J. Am. Chem. Soc.* **2009**, *131*, 7031–7039.
(30) Butt, H. J.; Franz, V. *Phys. Rev., E* **2002**, *66*, 031601.
(31) Loi, S.; Sun, G.; Franz, V.; Butt, H. J. *Phys. Rev., E* **2002**, *66*, 031602.
(32) Kunneke, S.; Kruger, D.; Janshoff, A. *Biophys. J.* **2004**, *86*, 1545–1553.
(33) Garcia-Manyes, S.; Oncins, G.; Sanz, F. *Biophys. J.* **2005**, *89*, 4261–4274.
(34) Leonenko, Z. V.; Finot, E.; Ma, H.; Dahms, T. E.; Cramb, D. T. *Biophys. J.* **2004**, *86*, 3783–3793.
(35) Garcia-Manyes, S.; Oncins, G.; Sanz, F. *Biophys. J.* **2005**, *89*, 1812–1886.
(36) Chiantia, S.; Ries, J.; Kahya, N.; Schwille, P. *ChemPhysChem* **2006**, *7*, 2409–2418.
(37) Sullan, R. M.; Li, J. K.; Zou, S. *Langmuir* **2009**, *25*, 12874–12877.
(38) Garcia-Manyes, S.; Sanz, F. *Biochim. Biophys. Acta* **2010**, *1798*, 741–749.

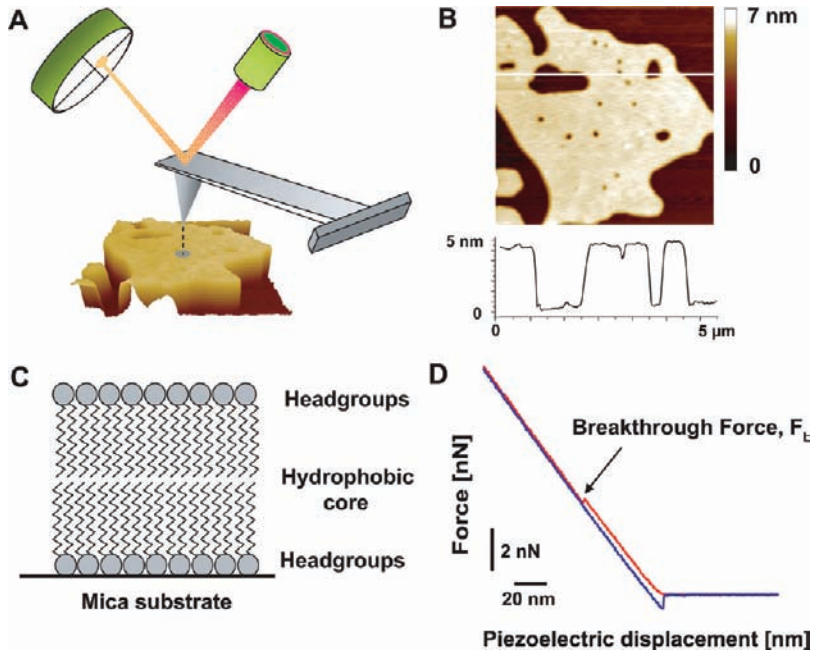

Figure 1. Rupture force of a SLB using an AFM tip is a clear molecular fingerprint. (A) Schematics of the experimental AFM setup. SLB micrometer-sized islands are first identified using tapping mode imaging. Force curves are then conducted in the center of such bilayers. (B) $5 \times 5\ \mu m^2$ image of a DMPC bilayer, revealing an expected thickness of ~5 nm (C). (D) Typical force curve on a SLB. In a typical cycle, the cantilever tip approaches the bilayer (red trace) up to a set maximum force. The piezoelectric is subsequently retracted (blue trace). During the approaching part of the cycle, the AFM tip applies an increasing *pushing* force on the bilayer. The bilayer is first elastically deformed, until a sudden jump appears, which marks the plastic penetration of the AFM tip through the lipid bilayer. The force value at which such a breakthrough event occurs, F_b, is strongly dependent on the chemical composition of the lipid bilayer.

The mechanical properties of each independent bilayer are tested by conducting force curves (Figure 1D) at a constant piezoelectric velocity of 1 μm s^{-1} under physiological ion strength conditions (150 mM NaCl, 20 mM $MgCl_2$, pH 7.4)[35] on the membrane center region, which exhibits a mechanical response different than in the case of the bilayer rim.[39] The resulting force−distance traces reveal a well-defined jump, measuring ~5 nm, and occurring at several nN of force. Such breakthrough event marks the penetration of the AFM tip through the SLB, identifying the onset of the plastic deformation regime (Figure 1D). In order to ensure that the main contribution of the force required to pierce the bilayer mainly arises from the mechanical resistance of the bilayer and not from the electrostatic interaction between the bilayer surface and the cantilever tip, we independently measured the DLVO forces arising between the probed bilayers with distinct chemical composition and the silicon nitride tip used in our experiments (see Supporting Information and Figure SI1). As observed in Figure SI1B (Supporting Information), the maximum repulsive forces measured at 0 separation are always lower than 100 pN, which is a vanishingly small value compared to the measured values for bilayer penetration, in the order of several nN. These results thus conclude that the high forces required to plastically deform the membranes mainly arise from the mechanical resistance of the membranes. Interestingly, the force at which the breakthrough occurs, F_b, does not significantly change between small-corrugated substrates such as SiO_2 or the atomically flat mica substrates used in the present work.[40] Akin to the unfolding force in single protein mechanical experiments,[41] the breakthrough force value unambiguously fingerprints the (nano)mechanical resistance of the probed supported membrane before being indented. In the present case, however, the cantilever tip *pushes* the sample, instead of *pulling* it as it is the case for the unfolding of a single polyprotein. It is therefore conceivable that the tip radius has a major effect on the F_b value.[42] In order to test this hypothesis, we measured the rupture force of the same DPPC bilayer using a cantilever tip in which the radius has been modified (Figure SI2, Supporting Information). These results demonstrate that, contrary to what has been reported in previous studies,[43] the tip radius has a vanishingly small effect on the F_b value, probably due to the brittle character of the membrane. Thus, F_b (and not the load) provides an unambiguous signature of the mechanical resistance of the bilayer at the nanometer scale. These results offer an experimental platform to quantitatively test the effect of the phospholipid chemical composition on the mechanical stability of a single supported membrane. In particular, our experiments aim at dissecting the partial role of each phospholipid moiety (polar headgroup and apolar chain) on the overall resilience of the supported membrane.

Effect of the Tail Length on the Bilayer (Nano)Mechanical Stability. We begin our experiments by testing the effect of the hydrophobic chain length on the breakthrough force. Figure 2 shows the AFM images of four distinct phospholipids bilayers that share the same PC headgroup and differ

(39) Nussio, M. R.; Oncins, G.; Ridelis, I.; Szili, E.; Shapter, J. G.; Sanz, F.; Voelcker, N. H. *J. Phys. Chem. B* **2009**, *113*, 10339–10347.
(40) Garcia-Manyes, S.; Oncins, G.; Sanz, F. *Electrochim. Acta* **2006**, *51*, 5029–5036.
(41) Carrion-Vazquez, M.; Oberhauser, A. F.; Fowler, S. B.; Marszalek, P. E.; Broedel, S. E.; Clarke, J.; Fernandez, J. M. *Proc. Natl. Acad. Sci. U.S.A.* **1999**, *96*, 3694–3699.
(42) Fraxedas, J.; Garcia-Manyes, S.; Gorostiza, P.; Sanz, F. *Proc. Natl. Acad. Sci. U.S.A.* **2002**, *99*, 5228–5232.
(43) Franz, V.; Loi, S.; Muller, H.; Bamberg, E.; Butt, H. H. *Colloids Surf., B* **2002**, *23*, 191–200.

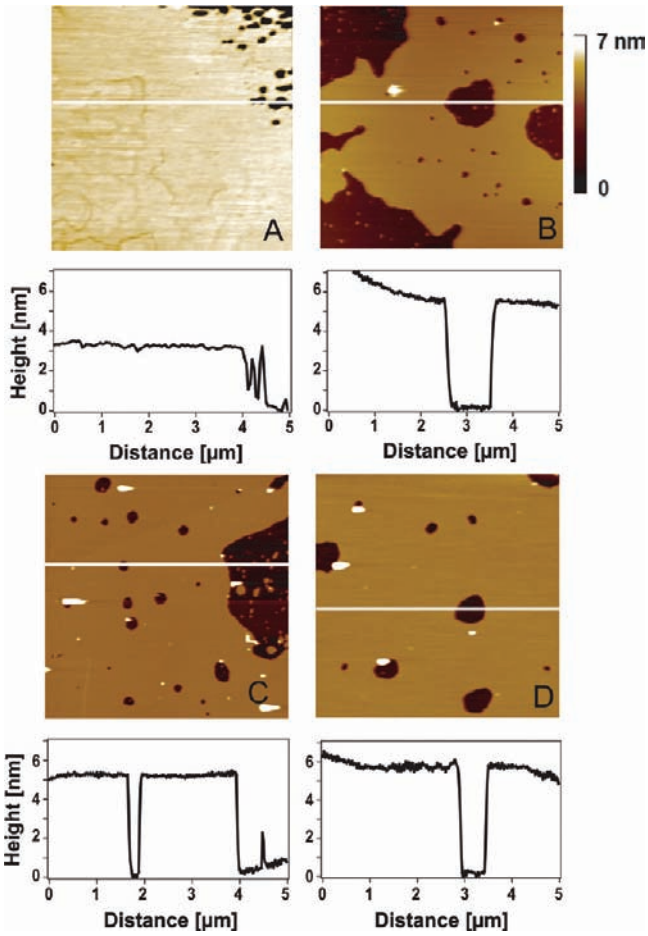

Figure 2. AFM images of PC phospholipid bilayers with different chain lengths reveal micrometer-size supported lipid bilayers. $5 \times 5\ \mu m^2$ tapping mode images of a supported lipid bilayer of DMPC (A), DPPC (B), DSPC (C), and DAPC (D). The cross-section profiles for each figure reveal a bilayer thickness of ~4−5 nm.

in the length of the hydrocarbon tails, spanning from 14 methylene groups (DMPC) up to 20 (DAPC). Their chemical structures are shown in Figure 3A. Noteworthy, only phospholipids that are in the solid phase at room temperature are compared, since the mechanical stability of the SLBs is significantly reduced close to the phase transition temperature, or when the lipids are in the liquid phase.[33] The distribution of breakthrough forces in each case is shown in Figure 3B. It is apparent from the histograms that the F_b value increases with the length of the hydrophobic chain. From the Gaussian fits to the data (dotted gray lines) we obtain the average rupture force for each distinct bilayer. These results are plotted as a function of the number of carbon atoms present in the hydrocarbon tail (Figure 3C). The slope of the linear fit to the data (dF/dC) indicates that, on average, increasing each hydrocarbon tail by 2 extra $-CH_2-$ groups results in ~6.6 nN increase of the F_b value. As a further control to validate the precision of our experimental approach, we measured the F_b values corresponding to mixtures of DMPC and DPPC bilayers of varying compositions (Figure SI3, Supporting Information), showing that there is a linear relationship between the amount of DMPC in the mixture and the decrease of F_b (Figure SI3B, Supporting Information). As described above, all our experiments are conducted under physiological ion strength conditions (150 mM NaCl, 20 mM $MgCl_2$, pH 7.4). Divalent cations (e.g., Mg^{2+} and Ca^{2+}) are known to enhance bilayer deposition onto hydrophilic surfaces.[35,40,44−46] Moreover, they bridge lipid polar heads,[47,48] thereby enhancing the mechanical resistance of the supported lipid bilayer.[35] It is most likely that the effect of divalent cations on the mechanical stability, once the bilayer is compact and well formed, is mostly determined by the enhanced bridging between neighboring phospholipid headgroups. However, the possibility that the headgroup−substrate interaction can further affect the disorder between the inner and the outer leaflets,[13,49] thus influencing the mechanical stability of the bilayer, cannot be ruled out. In order to address this question, we have conducted the mechanical experiments on the series of PC phospholipids with different chain lengths in a solution depleted of Mg^{2+}. As expected (Figure 3C, gray points), the mechanical stability of each bilayer is diminished with respect to the same bilayer measured in the presence of 20 mM Mg^{2+}. Of note, the trend showing the increase in the bilayer mechanical stability with the chain length is also observed in the absence of $MgCl_2$, thus demonstrating that the presence of $MgCl_2$ does not entail a significant variation in the measured trend for the bilayer nanomechanical resistance.

In order to further investigate the microscopic parameters defining the physicochemical state of the membrane we use the continuum nucleation model.[30,31] According to this model, the distribution of breakthrough forces required to create a hole under the cantilever tip is intimately related to the line tension, Γ, which represents the free energy associated with the unsaturated bonds of the molecules at the periphery of the hole, and with the effective spreading pressure, S, which is used to quantify the tendency of the film to spread into the gap between the tip and the substrate. Although the model oversimplifies the molecular nature of the system in that the film is considered a liquid in the lateral dimension, it has been shown to provide realistic quantitative numbers to explain indentation experiments on supported substrates under different conditions.[36,50] Under constant velocity conditions, the continuum nucleation model can be described by:

$$\ln P = -\frac{A}{K\upsilon}\int_{F_S}^{F}\exp\left(-\frac{c}{F'-F_S}\right)dF' \qquad (1)$$

$$c = \frac{2\pi^2\Gamma^2 R}{k_B T}$$

$$F_S = 2\pi RS$$

where A can be approximated to the resonance frequency of the cantilever, Γ is the line tension, k_B is the Boltzmann constant, T is the temperature, S is the spreading pressure and R and K are the radius and spring constant of the AFM cantilever tip,

(44) Jass, J.; Tjarnhage, T.; Puu, G. *Biophys. J.* **2000**, *79*, 3153–3163.
(45) Egawa, H.; Furusawa, K. *Langmuir* **1999**, *15*, 1660–1666.
(46) Kim, Y. H.; Rahman, M. M.; Zhang, Z. L.; Misawa, N.; Tero, R.; Urisu, T. *Chem. Phys. Lett.* **2006**, *420*, 569–573.
(47) Bockmann, R. A.; Hac, A.; Heimburg, T.; Grubmuller, H. *Biophys. J.* **2003**, *85*, 1647–1655.
(48) Bockmann, R. A.; Grubmuller, H. *Angew. Chem., Int. Ed.* **2004**, *43*, 1021–1024.
(49) Ramirez, D. M.; Ogilvie, W. W.; Johnston, L. J. *Biochim. Biophys. Acta* **2010**, *1798*, 558–568.
(50) Garcia-Saez, A. J.; Chiantia, S.; Salgado, J.; Schwille, P. *Biophys. J.* **2007**, *93*, 103–112.

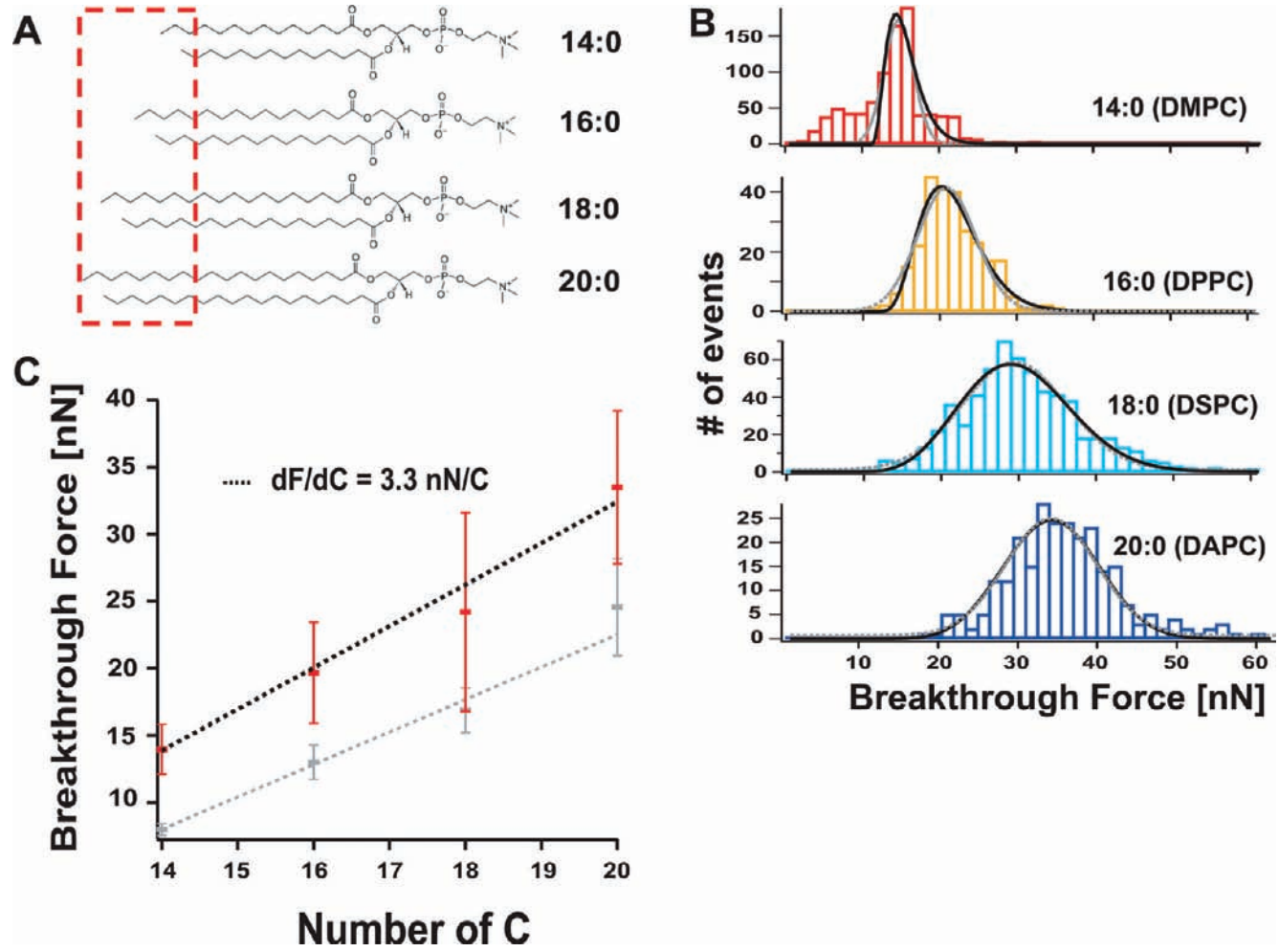

Figure 3. The mechanical resistance of the lipid bilayer is highly dependent on the length of the phospholipid tail. (A) Chemical structures of the tested PC phospholipids. The red square highlights the difference in the chain length. (B) Distribution of F_b values for the probed PC phospholipids with varying lengths. Gaussian fits to the data (dotted gray lines) yield a mean F_b value of 13.95 ± 1.87 nN, $n = 889$, DMPC (red); 19.66 ± 3.78 nN, $n = 266$, DPPC (orange); 24.2 ± 7.4 nN, $n = 1796$, DSPC (green); 33.5 ± 5.7 nN, $n = 263$, DAPC (blue). Fits to the continuum nucleation model (eq 2) are represented as solid black lines. (C) Plot of the measured average F_b value as a function of the number of carbons present in each phospholipid chain (red data points). Linear fit to the data (dotted line) yields a slope of 3.3 nN/-CH_2− moiety. Gray data points stand for the average F_b value for the probed phospholipids under 150 mM NaCl in the absence of Mg^{2+}.

respectively. Equation 1 can be integrated analytically and dP/dF can be calculated using:

$$\frac{dP}{dF} = \frac{A}{Kv}\exp\left\{-\frac{c}{F - F_S} - \frac{A}{Kv}\left[\exp\left(-\frac{c}{F - F_S}\right)(F - F_S) - cEi\left(\frac{c}{F - F_S}\right)\right]\right\} \quad (2)$$

$$Ei = \int_x^\infty \frac{e^{-t}}{t}dt$$

Fitting eq 2, with three floating parameters, to the experimental force distributions obtained for the probed PC phospholipids with varying chain length (black continuous lines in Figure 3B) allows calculation of the values for the line tension, Γ, and the spreading pressure, S. Figure 4A and Figure 4B show the variation of Γ and S as a function of the length of the hydrocarbon chain, respectively. While the values for the spreading pressure do not significantly vary with the chain length (which is an expected result since all phospholipids exhibit the same PC headgroup), the line tension increases linearly with the length of the hydrophobic tail. Similar to the results obtained for the mechanical stability, linear fit to the data (dotted line, Figure 4A) results in an increase of 5.4 pN for each extra −CH_2− group in the chain. It is surprising that the value of the line tension, Γ, which represents a direct measurement of the interaction between neighboring lipid molecules, is significantly dependent on the chain length. Indeed, one would expect that only the outer part of the molecules (i.e., the headgroups) would have an effect on the line tension. Two possible interpretations arise from our results; either the length of the hydrophobic chain contributes to a better packing of the overall membrane, thus enhancing the interaction between the neighboring zwitterionic PC headgroups, or alternatively the line tension is not strictly defined by the headgroups, in which case the length of the whole phospholipid molecule would contribute to the measured free energy of the molecules defining the periphery of the whole.

Next, we aim at investigating the effect of chain branching on the mechanical resilience of the bilayer. To this end, we compare the mechanical properties of the linear dipalmitoylphosphatidylcholine (DPPC) with its analogous branched phospholipid, diphytanoylphosphatidylcholine (DPhPC), Figure 5A. The distribution of breakthrough forces shown in Figure 5B demonstrates that, while DPPC exhibits a F_b value of ∼20

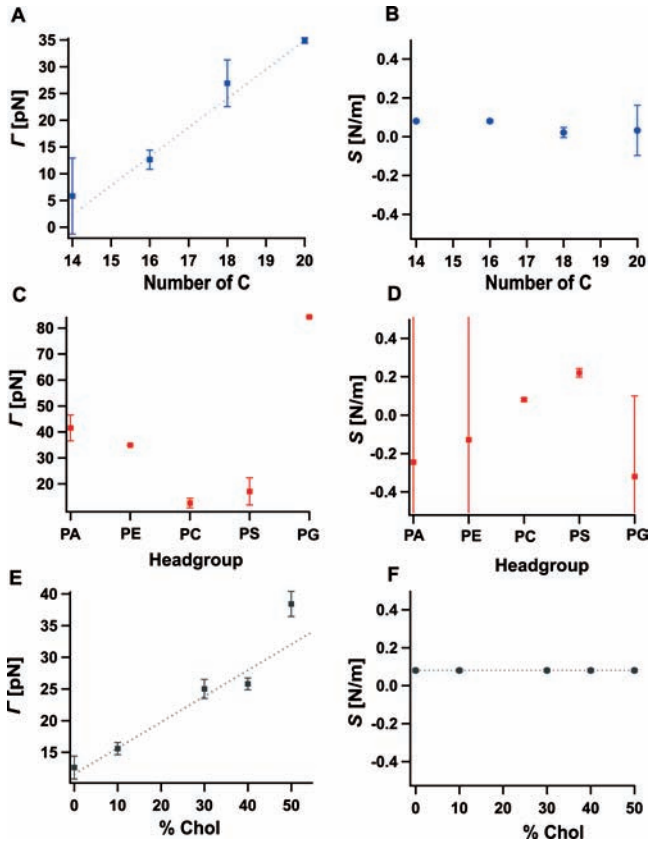

Figure 4. Fitting parameters of the continuum nucleation model. (A, B) Variation of the line tension, Γ, and spreading pressure, *S*, as a function of the length of the hydrocarbon chain, respectively. Linear fit in (A) yields a slope of 5.4 pN/ $-CH_2-$ group in the chain. (C, D) Dependency of Γ and *S* on the chemistry of phospholipid headgroup. (E, F) Variation of the line tension, Γ for a constant spreading pressure $S = 0.08 \pm 0.008$ N/m, as a function of cholesterol content on a DPPC bilayer. Linear fit (E) yields a slope of 0.4 pN/% cholesterol.

nN, the analogous branched DPhPC breaks at a much lower force of ∼12 nN, revealing the drastic effect of the lateral $-CH_3$ groups on the molecular packing of the bilayer. Interestingly, fitting the distribution of breakthrough forces to the continuum nucleation model, eq 2 (black lines in Figure 5B), results in a decrease of the line tension value from 12.6 ± 1.8 pN for DPPC down to a value of 9.8 ± 1.4 pN in the case of the branched DPhPC.

Effect of Unsaturations. Natural membranes are mainly composed of phospholipids with a high content of chain unsaturations. Polyunsaturated bilayers are characterized by low temperatures for the main-phase transition, which induces fluidity under physiological conditions. In order to systematically investigate the nanomechanical effect of the $-$*cis* double bonds present in the acyl chains, we compare the force required to penetrate a bilayer composed of phospholipids exhibiting respectively 1,2 and 3 unsaturations in their chains (Figure 6A, red squares). The histograms containing the distribution of F_b values for each particular bilayer (Figure 6B, red histograms) readily show an inversely proportional trend between mechanical stability and number of unsaturations (Figure 6C). From the linear fit to the data (red squares) we measure that, upon introduction of one additional unsaturation in each acyl chain, the breakthrough force is decreased by ∼4.6 nN. Interestingly, introducing an asymmetric unsaturation (Figure 6A, blue square) results in an even further mechanical destabilization, as demonstrated by the blue data point in Figure 6C. This observation confirms that asymmetric introduction of unsaturations in the phospholipid acyl chain results in an enhanced distortion of the molecular packing of the membrane.

Effect of Headgroup. The results presented above can be easily rationalized mostly according to the enhanced van der Waals attraction that originates between neighboring molecules while increasing their chain length (see Discussion section below). By contrast, predicting the effect of the headgroup chemistry on the membrane packing properties seems to be a much complex task, since the precise hydration properties of each particular headgroup,[51,52] together with their preferential ionic adsorption,[35] makes each case particular. In order to decipher whether the mechanical properties of the bilayer are only influenced by the hydrophobic tails or if, on the contrary, the polar headgroups also play a critical role in the membrane compactness, we measured the F_b values for a series of bilayers composed of phospholipids with the same chain length (16:0) and different headgroups, all of them in the gel phase. Figure 7 shows AFM images of the studied supported bilayers, and their chemical composition is highlighted in Figure 8A. The distribution of breakthrough forces for each probed phospholipid is shown in Figure 8B. Remarkably, the F_b value is greatly dependent on the phospholipid headgroup, ranging from $F_b \approx$ 3 nN for DPPA to $F_b \approx 66$ nN for DPPG. Figure 8C shows that the distribution of F_b values increases in the order PA < PE < PC < PS < PG. As before, the absence of Mg^{2+} decreases the mechanical stability of DPPS and DPPG, albeit keeping the same mechanical trend measured in the presence of $MgCl_2$ (Figures SI4 and SI5, Supporting Information). These results demonstrate the unexpected and significant effect of the phospholipid headgroup on the mechanical stability of the membrane. In contrast to the linear increase of the line tension obtained with increasing the chain length (Figure 4A), fitting the continuum nucleation data to the measured force distributions (Figure 8B, black continuous line) results in a significant variation in both the line tension and the spreading pressure for the probed bilayers with distinct headgroup chemistry (Figure 4C and 4D).

Effect of Cholesterol. Cholesterol (Chol) is a crucial constituent of eukaryotic cell membranes. It is mainly located in the plasma membrane and constitutes up to 40 mol % of the membrane lipids.[53] In particular, cholesterol is known to be one of the most important regulators of lipid organization, and mammals have developed sophisticated and complex mechanisms to maintain its cellular level within a narrow range.[54] Perhaps the most outstanding function of Chol is to crucially modulate the physical properties of biomembranes;[55] it increases their mechanical strength, thereby reducing passive permeability of water and small solutes, and it regulates membrane fluidity and phase behavior.[56] From the molecular perspective, cholesterol, due to the effect of its rigid ring system (Figure 9A) induces ordering and condensing effects to fluid phase lipids

(51) Cheng, J. X.; Pautot, S.; Weitz, D. A.; Xie, X. S. *Proc. Natl. Acad. Sci. U.S.A.* **2003**, *100*, 9826–9830.
(52) White, S. H.; King, G. I. *Proc. Natl. Acad. Sci. U.S.A.* **1985**, *82*, 6532–6536.
(53) Pasenkiewicz-Gierula, M.; Rog, T.; Kitamura, K.; Kusumi, A. *Biophys. J.* **2000**, *78*, 1376–1389.
(54) Maxfield, F. R.; Tabas, I. *Nature* **2005**, *438*, 612–621.
(55) Pan, J.; Mills, T. T.; Tristram-Nagle, S.; Nagle, J. F. *Phys. Rev. Lett.* **2008**, *100*, 198103.
(56) Rog, T.; Pasenkiewicz-Gierula, M.; Vattulainen, I.; Karttunen, M. *Biochim. Biophys. Acta* **2009**, *1788*, 97–121.

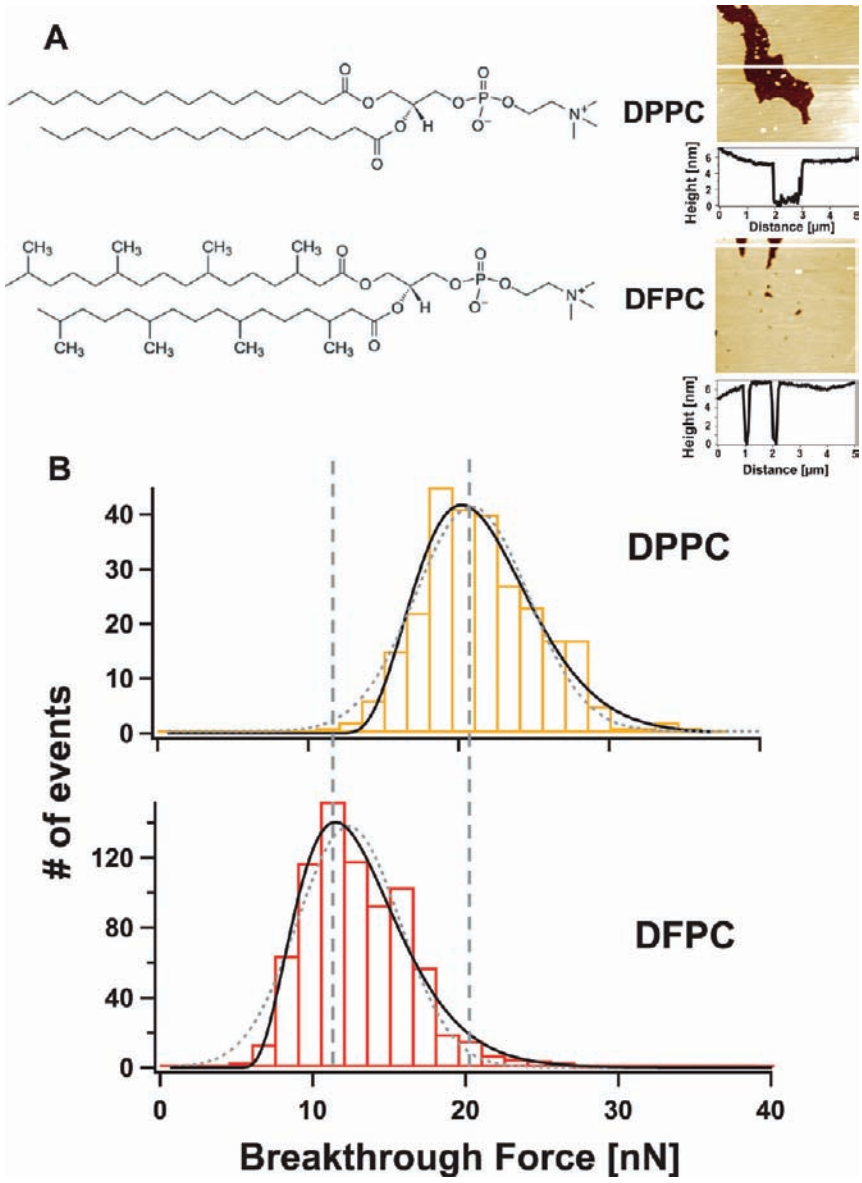

Figure 5. Chain branching has a significant effect on the mechanical stability of supported lipid bilayers. (A) Chemical structures of DPPC and DPhPC phospholipids. Inset: $5 \times 5\ \mu m^2$ AFM images with their corresponding cross-section profiles of the mica-supported lipid bilayers. (B) Distribution of breakthrough forces for DPPC (orange histogram), yielding a mean rupture force of 19.66 ± 3.78 nN ($n = 266$), and for the branched counterpart DPhPC (red histogram), yielding a mean rupture force of 11.61 ± 3.36 nN ($n = 778$). Dotted gray lines represent Gaussian fits to the data, whereas fits to the continuum nucleation model (eq 2) are shown as solid black lines. These results highlight the significant effect of the chain branching on the mechanical stability of chemically similar phospholipid bilayers.

forming the membrane,[57] while it has the reverse effect on phospholipids present in the gel phase.[56,58] Despite such assumed universal behavior, recent experiments have highlighted the different effect of cholesterol depending on the molecular structure of the neighboring lipids, and in particular, to the degree of chain unsaturation, the length of the hydrophobic tail and the different headgroup chemistry.[55,59] Indeed, the complex (and still poorly understood[60]) molecular interactions occurring between cholesterol and the rest of the membrane constituents have triggered a myriad of theoretical studies, most of them using molecular dynamics simulations.[53] Consequently, the subtle molecular role that cholesterol plays on regulating the biophysical properties of membranes invites experimental verification at the nanometer scale.

We have investigated the mechanical response to nanoindentation of a DPPC bilayer (gel phase, $T_m = 41$ °C) and a DLPC bilayer (liquid phase, $T_m = -1$ °C) as a function of cholesterol content. Figure 9B shows the distribution of F_b values for a DPPC SLBs containing an increasing amount of cholesterol, ranging from 0% up to 50%. AFM images of the probed surfaces are shown in Figure SI6 (Supporting Information). The distribution of breakthrough forces increases with the cholesterol concentration, ranging from ~20 nN at 0% Chol to ~60 nN at 50% Chol (the maximum physiologically relevant amount). The same trend is observed in the case of the DLPC bilayer (Figure SI7, Supporting Information). The average F_b

(57) Hung, W. C.; Lee, M. T.; Chen, F. Y.; Huang, H. W. *Biophys. J.* **2007**, *92*, 3960–3967.
(58) Vist, M. R.; Davis, J. H. *Biochemistry* **1990**, *29*, 451–464.
(59) Mills, T. T.; Huang, J.; Feigenson, G. W.; Nagle, J. F. *Gen. Physiol. Biophys.* **2009**, *28*, 126–139.
(60) Bennett, W. F.; Maccallum, J. L.; Hinner, M. J.; Marrink, S. J.; Tieleman, D. P. *J. Am. Chem. Soc.* **2009**, *131*, 12714–12720.

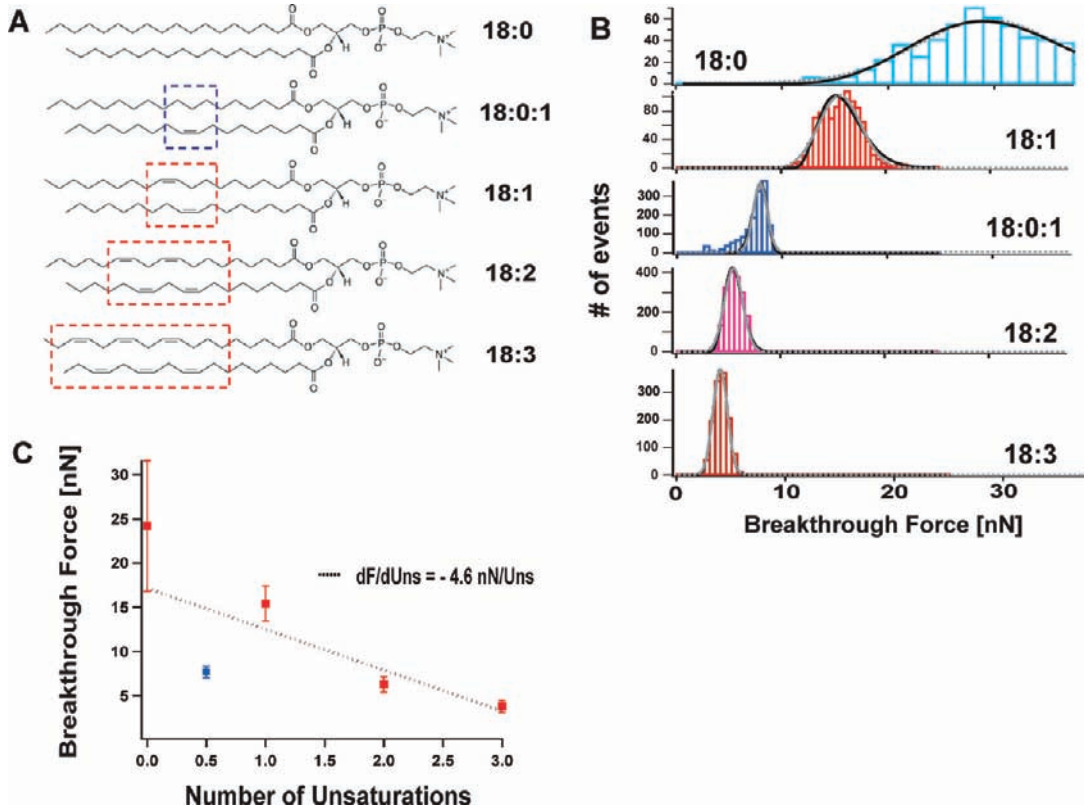

Figure 6. Mechanical resistance of the lipid bilayer depends on the number of unsaturations present in the hydrophobic tail. (A) Chemical structures of the probed phospholipids. Red squares mark the number and position of the symmetric unsaturations within the phospholipid structure. Blue square highlights the position of the asymmetric unsaturation in the case of 18:0−18:1 PC. (B) Distribution of F_b values for the probed phospholipids, where Gaussian fits to the data (dotted gray lines) yield a mean F_b value of 24.2 ± 7.4 nN, n = 1796, DSPC (18:0, green); 15.4 ± 2 nN, n = 1011, (18:1, red); 6.26 ± 0.87 nN, n = 1802, (18:2 red); 3.78 ± 0.66 nN, n = 1270, (18:3, red); 7.7 ± 0.66 nN, n = 1509, (18:0−18:1, blue). Fits to the continuum nucleation model (eq 2) are represented as solid black lines. (C) Plot of the measured F_b values as a function of the number of symmetric unsaturations present in each phospholipid chain. In the case of the asymmetrically unsaturated phospholipid (18:0−18:1, blue point) the unsaturation is represented as 0.5. Linear fit (dotted line) to the data corresponding to lipids exhibiting symmetric unsaturations (red data points) yields a slope of −4.6 nN/symmetric unsaturation. The blue data point (which is not included in the fit to the mechanical stability data for the bilayers exhibiting symmetric unsaturations) falls below the measured trend, highlighting the reduced mechanical stability promoted by the unsaturation.

value at each cholesterol concentration is plotted in Figure 9C. In the case of the DPPC bilayer, linear fit to the data indicates that the presence of each 1% of cholesterol increases its mechanical stability by ∼600 pN. Interestingly, no saturation at high Chol amounts is observed. This observation is in agreement with the results observed with the micropipet technique, in which K_a was found to saturate only above 60% Chol content.[61] The same trend is observed for the DLPC SLBs, even though with a smaller slope; in this case, increasing the cholesterol concentration by 1% results in an increase of 130 pN. These observations reveal the direct effect of cholesterol on the mechanical properties of the bilayer that, plausibly, reflect into bilayer molecular order. Such stiffening of the membrane upon cholesterol insertion is further confirmed when fitting the continuum nucleation theory (eq 2) to the distributions of breakthrough forces obtained at different cholesterol concentrations (continuous black line, Figure 9B). In these fits, the spreading pressure is kept fix to the S value obtained for the DPPC bilayer in the absence of cholesterol (S = 0.08 ± 0.008 N/m), Figure 4F. This is a realistic assumption according to Figure 4B and due to the fact that cholesterol is known to be in close contact with the hydrophobic region of the membrane.[62] The likewise resulting values for the variation of the line tension with cholesterol content are shown in Figure 4E. Akin to the results observed for the mechanical stability of the bilayer, the line tension increases linearly upon introduction of cholesterol. Linear fit to the data (dotted lines, Figure 4E) yields an increase of 0.4 pN/% cholesterol.

Discussion

Here we present the proof-of-principle of a complementary experimental approach that can be added to the toolbox of the existing biophysical techniques to quantitatively characterize the mechanics of supported lipid bilayers from the nanonewton/nanometer viewpoint.

Regarding the effect of the chain length on saturated, gel-phase PC phospholipids, our experiments reveal an increase of 3.3 nN in force per each additional $-CH_2-$ group present in the chain. Such an increase originates from a most favorable packing between neighboring hydrophobic chains. Indeed, it has been amply reported that long hydrocarbon tails interact better with each other than shorter ones. In particular, upon introduction of an extra $-CH_2-$ in the chain, the system's enthalpy increases by roughly 2 kJ/mol.[63] It is also plausible that the

(61) Needham, D.; Nunn, R. S. *Biophys. J.* **1990**, *58*, 997–1009.
(62) Chiu, S. W.; Jakobsson, E.; Mashl, R. J.; Scott, H. L. *Biophys. J.* **2002**, *83*, 1842–1853.
(63) Berg, J. M.; Tymoczko, J. L.; Stryer, L. *Biochemistry*; Freeman and Company: New York, 2007.

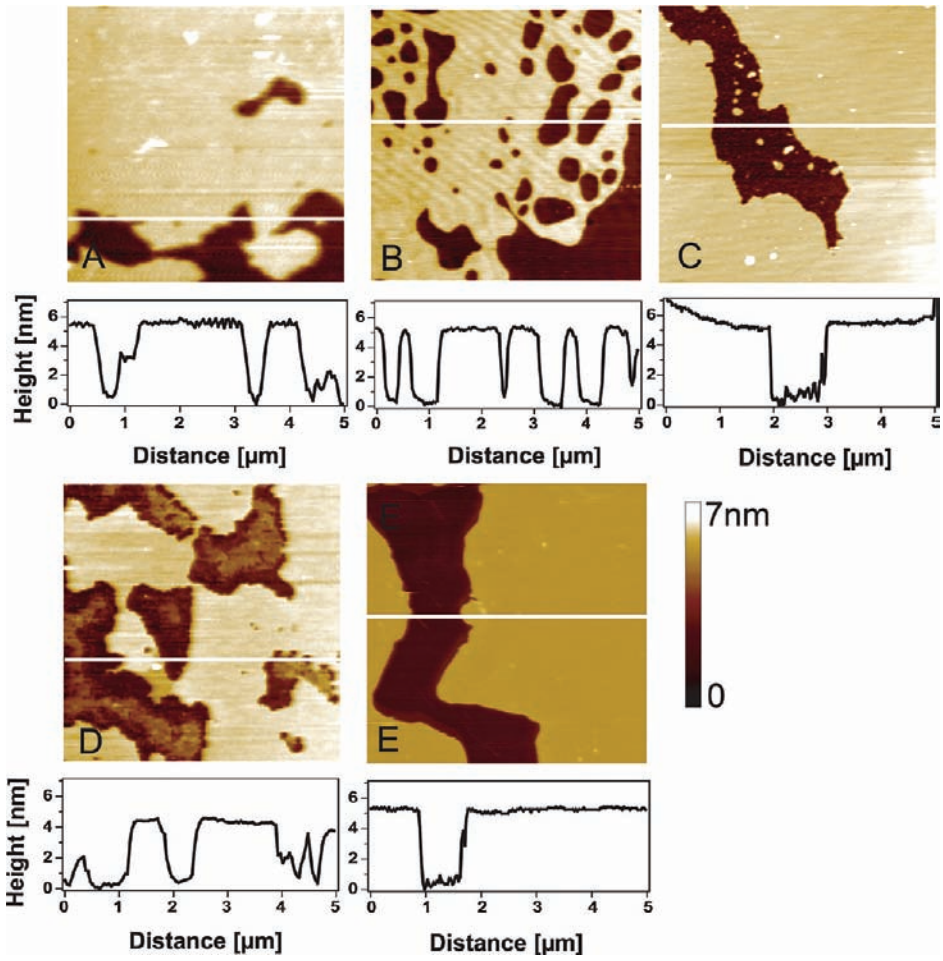

Figure 7. AFM images of phospholipid supported bilayers with different headgroup chemistries reveal micrometer-sized supported lipid bilayers. 5×5 μm^2 tapping mode images of a supported lipid bilayer of DPPA (A), DPPE (B), DPPC (C), DPPS (D) and DPPG (E). The cross-section profiles for each figure reveal an average bilayer thickness of ~4−5 nm.

entropic contribution connected with the increased hydrophobic interaction arising from the additional $-CH_2-$ groups present in the chain plays also a role in the increased mechanical resistance that we observe in our experiments. Furthermore, the introduction of a *−cis* double bond in the chain leads to a kink in the molecular structure. The resulting molecular tilt reduces the effective packing between molecules, giving rise to a lower melting temperature.[63] These observations correlate well with our observations that conclude that, as the number of chain unsaturations increases, the mechanical resistance of the bilayer is greatly reduced. In fact, bacteria regulate the fluidity of their membrane by varying the number of double bonds and length of the phospholipid hydrocarbon chains. Finally, we measured that molecular branching has also an outstanding effect on the SLBs mechanics. Synthetic model archaeal DPhPC exhibits a lower mechanical stability than its linear counterpart, DPPC. This observation can be rationalized in terms of the larger area per lipid for the branched DPhPC (76.8 $Å^2$) compared to that for the linear DPPC (62.0 $Å^2$), as revealed by molecular dynamics simulations conducted in the fluid phase.[64] Taken together, our results (Figures 3, 5 and 6) are in qualitative agreement with the vast and well-grounded textbook literature that correlates the physicochemical properties of membranes with the chemical composition of their phospholipid hydrophobic chains.[16] However, it is particularly revealing to observe how ensemble, thermodynamic quantities such as the melting temperature or the order parameter can be translated into the domain of mechanical stability. Our measurements highlight the dramatic impact that a fine chemical modification in the phospholipid tail has on the overall stiffness of the supported bilayer.

The findings regarding the mechanical implications of the headgroup chemistry are far less straightforward and highly unanticipated. The first striking observation is the huge range of forces required to indent the bilayer, spanning from ~3 nN (DPPA) all the way up to ~66 nN (DPPG). Second, there is a lack of correlation between the headgroup charge at neutral pH and the bilayer resilience; while the charged DPPA exhibits the lowest mechanical resistance, DPPS and DPPG show the highest mechanical stability (~40 nN and ~66 nN, respectively). Zwitterionic DPPE and DPPC fall into intermediate positions within the stability series (~9 nN and ~19 nN, respectively). In the case of hydrophobic chains, van der Waals forces mainly govern the interactions between neighboring chains. By contrast, the intermolecular forces that determine the molecular packing within hydrophilic headgroups are mainly electrostatic in origin, and also based on hydrogen bonding, both between neighboring molecules and with the surrounding solvent molecules. In general, the *a priori* expectation would be that in the case of charged phospholipids, the Coulombic repulsive interactions

(64) Shinoda, W.; Shinoda, K.; Baba, T.; Mikami, M. *Biophys. J.* **2005**, *89*, 3195–3202.

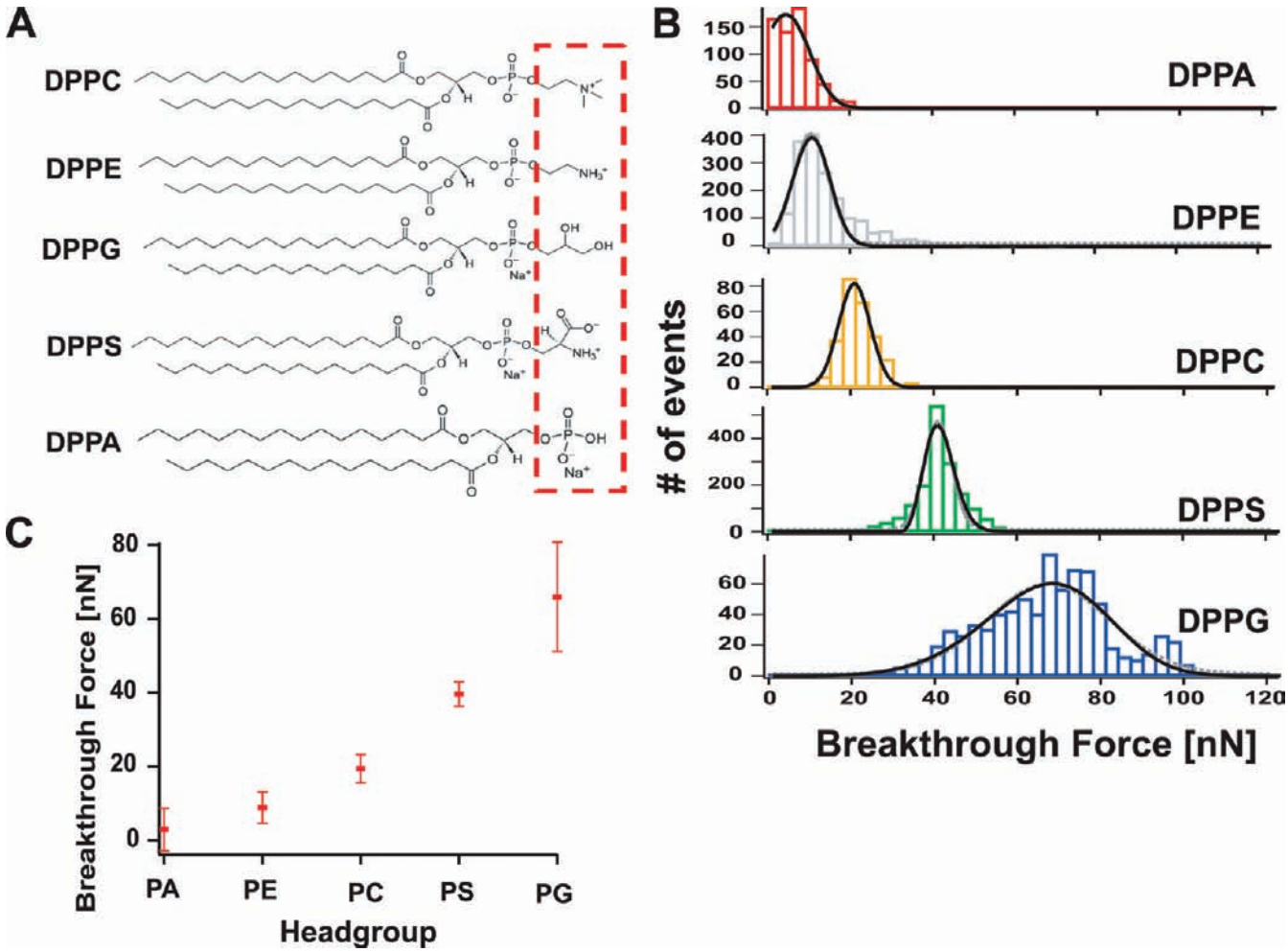

Figure 8. The mechanical resistance of the lipid bilayer is highly dependent on the chemistry of the phospholipid headgroup. (A) Chemical structures of the tested phospholipids exhibiting the same chain length (16:0) (B) Distribution of F_b values for the probed PC phospholipids with varying headgroups. Gaussian fits to the data (dotted gray lines) yield a mean rupture force of 2.99 ± 5.75 nN, n = 656, DPPA (red); 8.91 ± 4.26 nN, n = 1724, DPPE (gray); 19.66 ± 3.78 nN, n = 266, DPPC (orange); 39.57 ± 3.31 nN, n = 1623, DPPS (green); 65.91 ± 14.77 nN, n = 768, DPPG (blue). The reported errors stand for standard deviation obtained from the Gaussian fit to the data. Fits to the continuum nucleation model (eq 2) are shown as solid black lines. (C) Plot of the measured F_b values as a function of the headgroup.

between neighboring headgroups would lead to a bigger area per lipid, a lower degree of molecular packing and, therefore, to a lower mechanical stability. While this seems to be the case for DPPA, the results are indeed reversed for DPPS and DPPG. In the case of DPPS, molecular dynamics simulations have unexpectedly revealed that the area per lipid value for the charged DPPS is smaller (54.0 Å^2) than that for zwitterionic DPPC (62.0 Å^2), both calculated in the liquid phase.[65] Such a surprising discovery was accounted for either a strong coordination between DPPS molecules[65] or by a crucial effect of the Na^+ counterions,[66] which screen the repulsive negative charges induced by the serine group. In this sense, the specific adsorption of Na^+ cations makes the system akin to a model charged condenser with a diffuse double layer. Noteworthy, the force required to penetrate a DPPS bilayer (~ 40 nN) is very similar to that required to indent a solid alkali halide single fcc ionic crystal of NaCl or KCl (120−75 nN).[42] Although from the simulation viewpoint DPPG has deserved less attention, a similar interpretation regarding specific Na^+ adsorption would most likely apply to rationalize its enhanced mechanical stability. By contrast, DPPA has been described to exhibit the opposite behavior; upon adsorption of divalent cations such as Ca^{2+} or Ba^{2+} in micromolar concentrations, the bilayer undergoes a charge inversion phenomenon, ie., the total number of bound counterion charges exceeds the negative PA charge.[67] In our experiments, we employ 20 mM Mg^{2+} in the measuring solution. We speculate that such an overscreening effect that leads to an effective positive charge in the bilayer surface and thus to an electrostatic repulsion between neighboring groups, results in the reduced mechanical resilience that we measure (Figure 8). The relative results regarding DPPE and DPPC are also quite counterintuitive; while DPPE has shown to exhibit a lower area per lipid (42.9 Å^2)[68] than DPPC (47.9 Å^2),[69] it exhibits a lower mechanical stability (Figure 8). In particular, PE is known to exhibit a higher headrgroup hydration than PC, which should enhance a tighter packing of neighboring molecules.[68] It is nonetheless plausible that the lower mechanical stability that

(65) Cascales, J. J. L.; dela Torre, J. G.; Marrink, S. J.; Berendsen, H. J. C. *J. Chem. Phys.* **1996**, *104*, 2713–2720.
(66) Pandit, S. A.; Berkowitz, M. L. *Biophys. J.* **2002**, *82*, 1818–1827.
(67) Faraudo, J.; Travesset, A. *Biophys. J.* **2007**, *92*, 2806–2818.
(68) Pimthon, J.; Willumeit, R.; Lendlein, A.; Hofmann, D. *J. Pept. Sci.* **2009**, *15*, 654–657.
(69) Nagle, J. F.; Tristram-Nagle, S. *Biochim. Biophys. Acta* **2000**, *1469*, 159–195.

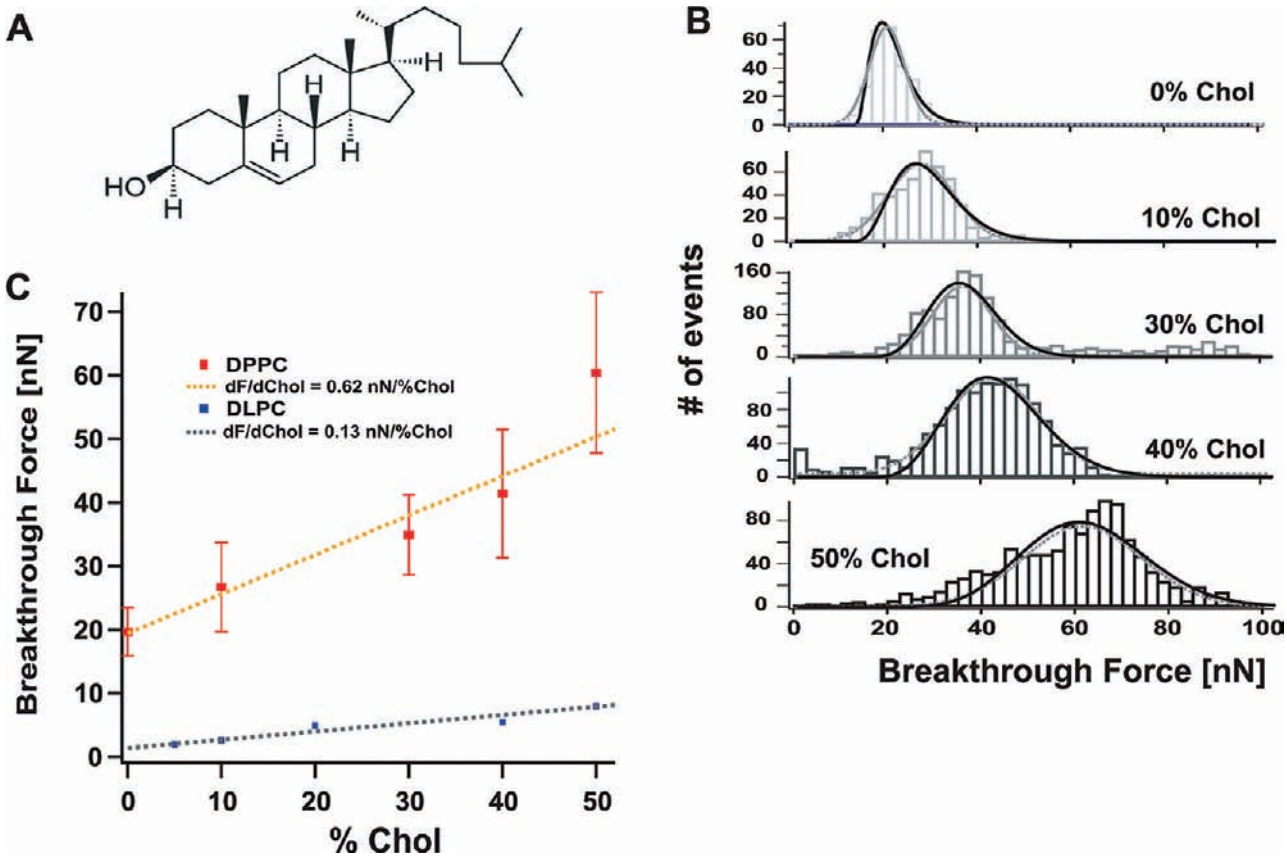

Figure 9. The presence of cholesterol induces stiffening of both liquid and gel phase SLBs. (A) Chemical structure of Chol. (B) Distribution of F_b values for DPPC SLBs with varying Chol concentrations. Gaussian fits to the data (dotted gray lines) yield a mean F_b value of 19.66 ± 3.78 nN, $n = 266$ (0% Chol); 26.71 ± 7.0 nN, $n = 481$, (10% Chol); 34.9 ± 6.29 nN, $n = 1291$, (30% Chol); 41.4 ± 10.04 nN, $n = 1671$, (40% Chol); 60.43 ± 12.62 nN, $n = 1124$, (50% Chol). The reported errors stand for standard deviation obtained from the Gaussian fit to the data. Fits to the continuum nucleation model (eq 2) are shown as solid black lines. (C) Plot of the mean F_b value as a function of the Chol concentration for DPPC (red data points). Linear fit to the data (orange dotted line) yields a slope of 620 pN/% Chol. In the case of DLPC (blue data points), linear fit to the data (dotted gray line) yields a slope of 130 pN/%Chol.

we measure for DPPE is due to the relative position of the headgroups within the subsurfaces, as demonstrated with monolayers; the higher the headgroup hydration (PE), the deeper the molecules embed themselves in the water surface to the detriment of monolayer cohesion.[70] Hence, PC headgroups induce better lateral intermolecular forces between phospholipids.[70] Our mechanical observations also agree with earlier mechanical experiments with AFM on lipid monolayers, which showed that the higher stored bending energy of PE compared to PC makes the PE monolayer easier to be plastically perturbed by the AFM tip.[71] Here it is interesting to consider that the observed difference in the mechanical stability between the different bilayers with distinct headgroups may arise from the temperature distance between the measuring temperature and the melting temperature in each case. This assumption would assume, at least in the gel phase, that there is a mechanical modulation within the same phase as a function of the temperature, in agreement with previous results.[33] Taken together, our results demonstrate the surprisingly crucial role that phospholipid headgroups play on the molecular cohesion of the bilayer.

Finally, our measurements reveal a dramatic and unanticipated effect of cholesterol on the mechanical stability of the supported membranes. In the case of DLPC, Chol induces a significant increase in the force required to puncture the membrane. Indeed, the mechanical stability at 50% Chol exhibits a 4-fold increase compared to that of pure DLPC. Such an increase in the mechanical stability is likely to stem from the transition from liquid-crystalline phase to liquid-ordered (l_o) phase. The l_o phase is characterized by very close intermolecular spacing with long-range translational disorder but short-range orientational order, which results in reasonable lateral fluidity.[72,73] As a result, cholesterol induces an increase of the bending and area compressibility moduli, implying a global stiffening of the membrane,[55] which is consistent with the results that we obtained for DLPC. Conversely, addition of Chol to gel-phase phospholipids is thought to decrease their molecular lateral packing, since it triggers the mixture to also evolve from the gel phase toward the liquid-ordered phase.[56,74] In this respect, one would expect a decrease of the breakthrough force upon the addition of cholesterol to the gel-phase DPPC supported bilayer. Contrary to these expectations, our experiments clearly demonstrate that upon addition of Chol, DPPC SLBs are able to withstand much higher forces before breaking (Figure 9). It is indeed remarkable that the force required to penetrate the

(70) Anton, N.; Saulnier, P.; Boury, F.; Foussard, F.; Benoit, J. P.; Proust, J. E. *Chem. Phys. Lipids* **2007**, *150*, 167–175.
(71) Hui, S. W.; Viswanathan, R.; Zasadzinski, J. A.; Israelachvili, J. N. *Biophys. J.* **1995**, *68*, 171–178.
(72) Marsh, D. *Biochim. Biophys. Acta* **2010**, *1798*, 688–699.
(73) Tierney, K. J.; Block, D. E.; Longo, M. L. *Biophys. J.* **2005**, *89*, 2481–2493.
(74) Giocondi, M. C.; Yamamoto, D.; Lesniewska, E.; Milhiet, P. E.; Ando, T.; Le Grimellec, C. *Biochim. Biophys. Acta* **2010**, *1798*, 703–718.

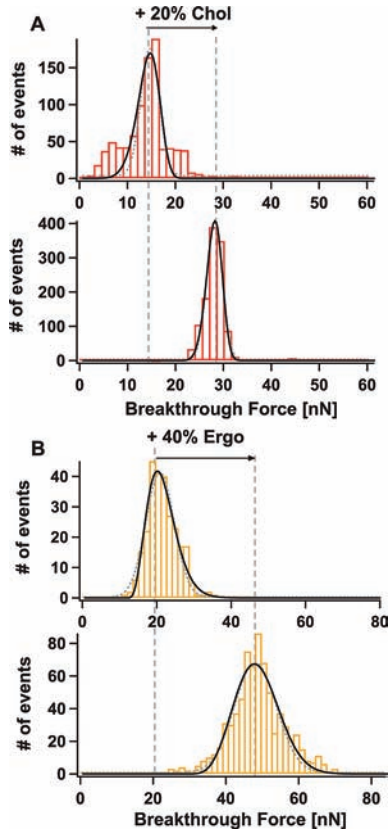

Figure 10. Cholesterol and ergosterol increase the mechanical stability of DMPC- and DPPC-supported lipid bilayers, respectively. (A) Distribution of F_b values for DMPC SLBs without (left) and with (right) the presence of 20% Chol. Gaussian fits to the data (dotted gray lines) yield a mean rupture force of 13.95 ± 1.87 nN, $n = 889$ in the absence of cholesterol, which increases up to a mean rupture force value of 27.40 ± 1.62 nN, $n = 1173$ in the presence of 20% Chol. (B) Distribution of F_b values for DPPC SLBs in the absence (19.66 ± 3.78 nN, $n = 266$, left) and presence (47.37 ± 5.75 nN, $n = 742$, right) of 40% ergosterol. The reported errors stand for standard deviation obtained from the Gaussian fit to the data. Fits to the continuum nucleation model (eq 2) are shown as solid black lines.

bilayer under 50% Chol (~60 nN) is 3-times higher than that for pure DPPC. Moreover, the linear trend of the breakthrough force with the Chol content contrasts with the nonlinear trend of the area compressibility modulus (K_a) observed for giant unilamellar vesicles using the micropipet aspiration technique.[61,73] In order to further study such unexpected increase of the mechanical stability of the gel-phase DPPC bilayer upon addition of cholesterol, we probed the effect of addition of 20% cholesterol on a DMPC bilayer. Similar to the results obtained for DPPC, the mechanical resistance of the bilayer increased by 50% upon addition of 20% cholesterol (Figure 10A). This result confirms that the stiffening effect of cholesterol seems to be a more general phenomenon that is not restricted to model DPPC SLBs, the "hydrogen atom[6]" of lipid membranes. Next, in order to investigate whether these results are specific to cholesterol or if they share commonality with other sterols, we studied the change in the mechanical properties of a DPPC bilayer upon the addition of 40% ergosterol. Ergosterol is the main sterol component of plasma membrane of lower eukaryotes, such as certain protozoa, yeast and other funghi, and of insects such as *Drosophila*.[73,75] From the molecular viewpoint, ergosterol is thought to promote an ordering effect similar or even higher to that of cholesterol.[56] Figure 10B shows that addition of 40% ergosterol increases the mechanical stability of DPPC from ~20 nN up to ~47 nN, thus demonstrating that the stiffening effect observed for cholesterol in gel-phase supported lipid bilayers is likely to be a general mechanism for different sterols. These results are consistent with the similar mechanical effects induced by cholesterol and ergosterol reported for giant unilamellar vesicles.[73] The origin of such unanticipated sterol-induced mechanical stiffening of gel-phase supported bilayers is still unknown. It is plausible that the gel/liquid-ordered transition is hampered by the effect of the supporting surface. In fact, the presence of a substrate has been shown to significantly alter the thermodynamic properties defining supported lipid membranes containing cholesterol.[76] Of note, our AFM images of the DPPC SLBs with varying concentrations of cholesterol do not reveal the presence of phase separation or nanodomains within the instrumental resolution (Figure SI6, Supporting Information). However, this result does not preclude the coexistence of both the gel and liquid-ordered domains, since the height difference for both phases should not be greater than ~5 Å and thus close to the technique resolution.[74] The putative surface effect certainly invites future verification by imaging the evolution of SLBs with temperature at different Chol concentrations, which would allow reconstruction of the phase diagram of binary phase mixtures in supported lipid bilayers[77] and compare it to the better established phase diagrams measured for free-standing bilayers.[72]

Interestingly, the interpretation of our results in terms of the continuum nucleation theory[30,31] gives rise to results that directly reflect the trends experimentally observed for the distribution of breakthrough forces under different chemical conditions. For example, we observe that, for the PC phospholipids with different chain lengths, the spreading energy remains approximately constant (same PC headgroup) while the line tension increases linearly with the length of the hydrophobic tail, similarly to the mechanical trend. Similarly, the value of line tension also diminishes with increasing the molecular branching of the hydrophobic tail. By contrast, both the spreading energy and the line tension significantly vary in a nonintuitive manner when changing the phospholipid headgroup moiety. Finally, upon addition of cholesterol to a DPPC supported bilayer, the line tension increases linearly with the cholesterol content, akin to the average yield threshold force. Altogether, these results demonstrate the qualitative agreement of the parameters extracted from the nucleation theory with the model-free nanomechanical trends observed in our experiments.

Conclusions

The experiments presented here provide the proof-of-principle of a novel quantitative experimental approach to the probe of the mechanical properties of supported lipid bilayers at the nanometer scale (Figure SI8, Supporting Information). Crucially, our results demonstrate the robustness of our experimental approach in providing physical parameters that are characteristic of the supported bilayer, and mostly independent of the AFM cantilever tip. Our experiments reveal a dramatic effect of the phospholipid chemical structure on the membrane mechanical stability. While presented here for model, synthetic membranes, these studies hold promise for being expanded to biologically

(75) Bloch, K. E. *CRC Crit. Rev. Biochem.* **1983**, *14*, 47–92.
(76) Stottrup, B. L.; Veatch, S. L.; Keller, S. L. *Biophys. J.* **2004**, *86*, 2942–2950.
(77) Vanegas, J. M.; Faller, R.; Longo, M. L. *Langmuir* **2010**, *26*, 10415–10418.

relevant membranes composed of a myriad of different phospholipids within a broad concentration range. In particular, extending these experiments to asymmetric bilayers,[78] to different sterol molecules,[73] to the insertion of membrane proteins,[50] or to more complex systems such as ternary mixtures, with the final long-term aim to identify the high chemical complexity of plasma membranes, will provide a general framework to understand the correlation between membrane chemical composition and phospholipid lateral organization. In principle, these experiments can pave the way to study the reverse engineering of different bilayers, in the sense that the mechanical resistance of the supported bilayer could eventually be designed *a priori* by combining the 'right' headgroup with the 'desired' chain length. Furthermore, comparing these results to supported bilayers in which the bilayer/support interaction is minimized would provide a direct measurement of the effect of the supporting surface on the nanomechanics of lipid bilayers. For example, the effect of the substrate corrugation,[12,13] of porous substrates,[39] or the use of tethered lipid membranes,[79] lipid membranes on a polymer cushion[28] or pore-spanning lipid bilayers[29]provide promising perspectives to study the effect of the substrate on the nanomechanical properties of the bilayers. Moreover, the effect of the interleaflet coupling, which is also highly influenced by the substrate and the physical parameters of the measuring system,[80] on the mechanical properties of the supported lipid bilayers deserves experimental investigation. From the physical perspective, the penetration of the cantilever tip into the bilayer has been modeled as a barrier limited two-state process. However, our experiments reveal that more than a single molecular determinant (tail, headgroup) is involved in the breakthrough process. Therefore, it would be of great interest to experimentally determine the width of the energy barrier(s) governing the system, Δx, which would provide a molecular counterpart able to map out in detail the length-scale of the molecular interactions that hold neighboring phospholipid molecules together. Such a fine determination begs for the utilization of the force-clamp technique, which has been shown to be particularly sensitive at determining the transition state structures of single proteins under the effect of a constant pulling force.[81] Furthermore, due to the nanometer-scale nature of our experiments, the experimental approach described here provides the ideal platform to bridge the gap with MD simulations, which uncover a variety of molecular mechanisms that are not accessible with mesoscopic experimental techniques.[56,82] Finally, from the technological viewpoint, these experiments will help in the design of tailored nanodevices that rely on the robustness of supported lipid bilayers.[83] To sum up, our results demonstrate the compelling effects of subtle structural variations of the chemical structure of phospholipid molecules on the behavior of supported lipid bilayers when exposed to mechanical forces, a mechanism of common occurrence in nature.

Acknowledgment. We thank Rodolfo Hermans (Columbia University) for help in data analysis and Pau Gorostiza (IBEC) for helpful discussions. S.G.-M. thanks the Generalitat de Catalunya, the Fundación CajaMadrid and the Fundación IberCaja for financial support. This work has been supported by the Ministerio de Educación y Ciencia (Spain) through the project CTQ2007-68101-C02-01 (to F.S.).

Supporting Information Available: Additional AFM imaging and force spectroscopy characterization of different membranes with distinct chemical composition. This material is available free of charge via the Internet at http://pubs.acs.org.

JA1002185

(78) Manno, S.; Takakuwa, Y.; Mohandas, N. *Proc. Natl. Acad. Sci. U.S.A.* **2002**, *99*, 1943–1948.
(79) Koper, I. *Mol. Biosyst.* **2007**, *3*, 651–657.
(80) Seeger, H. M.; Marino, G.; Alessandrini, A.; Facci, P. *Biophys. J.* **2009**, *97*, 1067–1076.
(81) Garcia-Manyes, S.; Dougan, L.; Badilla, C. L.; Brujic, J.; Fernandez, J. M. *Proc. Natl. Acad. Sci. U.S.A.* **2009**, *106*, 10534–10539.
(82) Berkowitz, M. L. *Biochim. Biophys. Acta* **2009**, *1788*, 86–96.
(83) Meister, A.; Gabi, M.; Behr, P.; Studer, P.; Voros, J.; Niedermann, P.; Bitterli, J.; Polesel-Maris, J.; Liley, M.; Heinzelmann, H.; Zambelli, T. *Nano Lett.* **2009**, *9*, 2501–2507.